JOURNAL OF MATERIALS SCIENCE **35** (2000) 71–77

DC extended arc plasma nitriding of stainless and high carbon steel

A. SAHU*‡, B. B. NAYAK*, N. PANIGRAHI*, B. S. ACHARYA*, B. C. MOHANTY*
*Regional Research Laboratory, Bhubaneswar 751013, India
‡Centre of Plasma Physics, Dispur, Guwahati 781006, India
E-mail: bijan_nayak@yahoo.com

Stainless steel (SS 302) and high carbon steel (HCS) substrates were nitrided in a pot type arc plasma furnace in the temperature range 1100–1200 °C under different gas (Ar, N_2, H_2) mixture configurations for twenty minutes each. The nitrided surfaces were characterized by XRD, SEM, metallography and microhardness. Depth of the nitride layer grown was found between 40 to 50 μm. Microhardness for SS 302 was observed to increase by about three to four times but for HCS the increase was not more than two times. The major compound phases to grow by this method were indentified to be $Fe_{2-3}N(\varepsilon)$, (Cr, Fe)N_{1-x} and CrN in case of SS 302 whereas for HCS the phases were recognised as $Fe_{2-3}N(\varepsilon)$, (Cr,Fe)N_{1-x}, $Fe_2N(\xi)$ and WN. Further details about the experiment and characterization of arc plasma nitrided steel are reported and discussed in this paper.

1. Introduction

Nitriding, basically a surface hardening process, produces improvements in wear and corrosion resistance, hardness and fatigue lifetimes of metals. Thus, iron and steel components, particularly engineering components, are often nitrided to prevent their premature failure due to progressive decay of surface materials by erosion, abrasion, corrosion etc. under extreme duty conditions.

The conventional nitriding processes adopted in industry use either cyanide-cyanate fused salt bath or gases like N_2 or NH_3 for obtaining case depth of various thicknesses (usually less than 0.5 mm). Due to the toxicity involved in cyanide-cyanate salt, its handling in industrial scale poses a major problem. Gas nitriding, on the other hand, requires relatively more time (usually in the range of several hours) for developing desired case depth. With a view to overcoming the drawbacks highlighted above, plasma nitriding has now come to centre-stage in industrial nitriding process. Besides being a clean and non-toxic process that involves considerably less nitriding time, a close control over the nature and structure of the nitrided layer is possible in plasma process [1–6]. The white brittle layer grown in all conventional nitriding processes does not appear in the plasma process. This is a significant advantage as the need to machine steel components in order to remove the white layer is avoided.

Though most commercial plasma nitriding reactors presently in operation use low pressure dc glow discharge plasma [7], interests have also grown in recent times in arc plasma nitriding [8] due to the following advantages: a) faster diffusion and reaction kinetics of the activated species on substrate surface, b) higher density of reactive species and c) reduced processing time. In the present work we have made an attempt to nitride two widely used engineering materials, namely, stainless steel (SS 302) and high carbon steel (HCS) in a pot type arc plasma furnace under different gas mixtures consisting of Ar, N_2 and H_2. The nitrided samples have been characterized by X-ray diffraction (XRD), metallography, scanning electron microscopy (SEM) and microhardness and the results are discussed to throw some light on high temperature nitriding phenomenon.

2. Experimental

The nitriding substrates were taken in the form of circular discs (25 mm dia, 3 mm thickness) for SS 302 and square plates ($12 \times 12 \times 3$ mm) for high carbon steel. The surfaces of the substrates were mechanically ground and polished first by silicon carbide paper (120, 320, 400 & 600 grit) and then by alumina slurry (1.0, 0.05 & 0.03 μm grade) to yield a mirror finish. The compositions of SS 302 and HCS are given in Table I.

The plasma nitriding furnace (Fig.1) is a vertical pot furnace indigenously designed and developed by the Special Materials Division of Regional Research Laboratory, Bhubaneswar. The furnace has provision to work both in transferred and non-transferred arc mode. Nitriding of substrate surfaces was carried out in the non-transferred mode in order to avoid melting of substrate. The hearth of the furnace constitutes of a salamander (clay bonded SiC) crucible insulated by bubble alumina. Another crucible made of graphite is fixed at the centre of the hearth and rests on a magnesia block at the bottom. The graphite crucible is laterally supported by a plurality of graphite rods (four numbers) which also act as electrical feed throughs. Graphite wool is filled into the intervening space of the hearth to provide

TABLE I Composition of SS 302 and HCS (wt %)

	SS 302	HCS
C	0.08–0.20	0.65–0.80
Cr	17.00–19.00	3.75–4.50
Mn	2.00	—
Ni	8.00–10.00	—
W	—	17.25–18.75
V	—	0.90–1.30
Mo	—	0.70
Fe	Balance	Balance

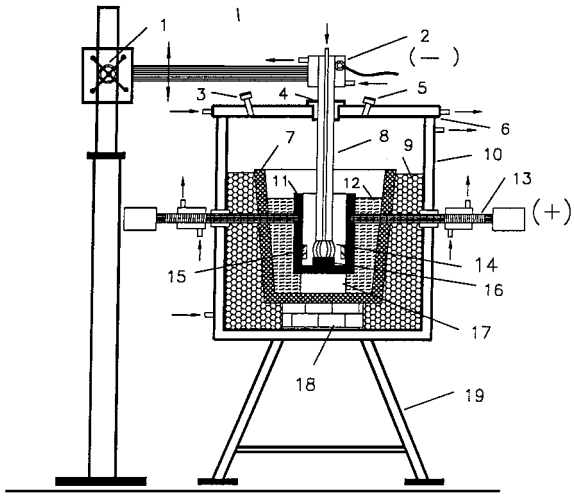

Figure 1 Schematic diagram of arc plasma nitriding furnace. (1) Rack and pinion, (2) electrode holder with water cooling, (3) gas exhaust outlet, (4) alumina bush with graphite sleeve, (5) viewing port, (6) water cooled steel cover, (7) salamander hearth, (8) graphite electrode, (9) bubble alumina, (10) water cooled steel casing, (11) graphite crucible, (12) graphite wool, (13) water cooled graphite electrode, (14) plasma, (15) nitriding substrate, (16) graphite block, (17) magnesia block, (18) alumina block, (19) supporting structure.

insulation. The inner vertical wall of the graphite crucible is coated with magnesia to prevent side arcing and reduce carbon contamination. A graphite electrode is vertically introduced into the graphite crucible from the top end to serve as cathode. The cathode has an axial hole to pass plasmagen gas (Ar, N_2, H_2) into the arc zone which is formed between the base of graphite crucible and the top electrode. The graphite rods in lateral configuration are normally kept at fixed positions while the top electrode is attached to a rack and pinion arrangement to provide upward and downward movement, thus changing the arc length as desired from time to time. The outer ends of the graphite support rods and the cathode were water cooled through copper holders. Exhaust gases and vapours are released through an outlet provided at the top end of the furnace. The cathode and the feed throughs were connected to the negative and positive polarity of a 35 KW power supply respectively. Further details of the furnace are illustrated in the diagram shown in Fig. 1.

The finely polished substrates were kept vertically by supporting against the magnesia coated wall of the graphite crucible. The substrates were treated with three types of plasma: (a) argon (b) argon + nitrogen (c) argon + nitrogen + hydrogen. The details of gas compositions are shown in Table II and III. As argon is

TABLE II Typical phases identified by XRD in SS 302 substrate surface after exposure to different plasmas

Plasma	Substrate temperature (°C)	Phase	
		Major	Minor
—	Room temp.	Austenite SS	—
Ar (vol. flow 1 l/min)	1205	Austenite SS	Fe_2O_3 (maghemite-Q) Fe_2O_3 (hematite) Fe_3O_4 (magnetite) $Fe_{2-3}N(\varepsilon)$
Ar-N_2			
Ratio 1 : 3	1150	$Fe_{2-3}N(\varepsilon)$	Fe_2O_3 (maghemite-Q)
by vol. 1 : 4	1120	$(Cr, Fe)_2N_{1-x}$	Fe_2O_3 (hematite)
flow 1 : 5	1075	CrN	
in l/min)			
Ar-N_2-H_2			
Ratio 1 : 1 : 3	1185	$Fe_{2-3}N(\varepsilon)$	Fe_2O_3 (maghemite-Q)
by vol. flow		$(Cr, Fe)_2N_{1-x}$	Fe_2O_3 (hematite)
(in l/min)		CrN	

TABLE III Typical phases identified by XRD in HCS substrate surface after exposure to different plasmas

Plasma	Substrate temperature (°C)	Phase	
		Major	Minor
—	Room temp.	Austenite HCS	—
Ar (vol. flow 1 l/min)	1195	Austenite HCS	Fe_2O_3 (maghemite-Q) Fe_2O_3 (hematite) $Fe_{2-3}N(\varepsilon)$
Ar-N_2			
Ratio 1 : 3	1145	$Fe_2N(\xi)$	Fe_2O_3 (maghemite-Q)
by vol. 1 : 4	1125	$(Cr, Fe)_2N_{1-x}$	Fe_2O_3 (hematite)
flow 1 : 5	1085	$Fe_{2-3}N(\varepsilon)$, WN	W_2N
in l/min)			
Ar-N_2-H_2			
Ratio 1 : 1 : 3	1180	$Fe_{2-3}N(\varepsilon)$	Fe_2O_3 (maghemite-Q)
by vol. flow		$(Cr, Fe)_2N_{1-x}$	Fe_2O_3 (hematite)
(in l/min)		Fe_2N, WN	

a monoatomic gas, it forms plasma at lower electrical excitation potential and thus maintains a stable plasma while plasma nitriding is carried out. Being inert, argon also prevents oxidation of substrate and does not affect the nitriding action in nitrogenous plasma. Hydrogen has been added in the gas mixture at the ratio $N_2 : H_2 = 1 : 3$ in order to form ammonia plasma. The following experimental conditions were maintained for plasma nitriding.

Arc length	:	1.0–1.5 cm
Arc voltage	:	40–50 V
Arc current	:	130–160 A
Gas flow rate	:	0.5–1.5 l/min
Plasma exposure time	:	20 min
Distance of arc centreline to the sample	:	3.5 cm

The arc length as above was maintained to produce relatively lower crucible wall temperature so that the substrates would not melt at the time of nitriding. The temperatures of the nitriding substrates were measured by focussing a Minolta IR pyrometer on the substrate surfaces through the viewing port provided on the top case of the furnace. X-ray

diffraction patterns of nitrided substrates were recorded by using an automatic Philips X-ray diffractometer (APD1710) having Bragg-Brentanno parafocussing geometry with vertical goniometer having attachments like autodivergence, receiving and scatter slits and curved graphite monochromator. The diffractometer was calibrated using SRM 640A silicon powder as an external standard. The identification of phases was performed using Hanawalt's search-match method. The surface microstructures of the substrates were viewed under a Leitz optical microscope and Jeol 35 CF scanning electron microscope. Vicker's microhardness numbers of nitride grains were determined by a Leitz-Wetzlar hardness tester at 100 g load using a diamond indentor.

3. Results

The ion temperature (or plasma temperature) measurement in thermal plasma is quite crucial in nitriding experiments. Our pyrometer measurement shows that the substrate temperature does not exceed 1200 °C in any case. The exact temperatures determined from our measurements are shown in Tables II and III. The XRD results of un-nitrided and arc plasma nitrided SS 302 and HCS substrates are also summarized in these Tables. In the case of SS 302, the austenite phase remains as the major phase after treatment with the first kind of plasma i.e. argon plasma. Minor amounts of different iron oxides along with the presence of a small amount of mixed nitride phase $Fe_{2-3}N$ are identified even if inert gas (argon) plasma medium was maintained. Three different ratios of Ar and N_2 were maintained in the second kind of plasma (Ar-N_2). Besides Fe_3N and CrN, mixed nitride of Fe and (Cr-Fe) are observed to occur as major phases and no austenite phase is seen to give any reflection. Two oxides such as maghemite and hematite are still marked to appear as minor phases. In the third kind of plasma i.e. ammonia plasma, except for the absence of Fe_3N, the occurence of major and minor phases are seen to be almost similar to that of Ar-N_2 plasma case. The typical phases observed in case of HCS are summarized in Table III which shows the total disappearance of austenite reflection after nitridation and the occurence of major relections due to Fe_3N, Fe_2N, WN and mixed phases of $Fe_{2-3}N$, $(Cr\text{-}Fe)_2N_{1-x}$ after treatment in either Ar-N_2 or Ar-N_2-H_2 plasma. Hematite and maghemite are seen to occur as minor phases along with Fe_3N and WN in some cases. Surprisingly no reflection due to any carbide or carbonitride is marked in any XRD of HCS.

Fig. 2a and b and Fig. 3a and b exhibit optical micrographs of the surface microstructures of SS 302 and HCS surfaces respectively in un-nitrided and nitrided

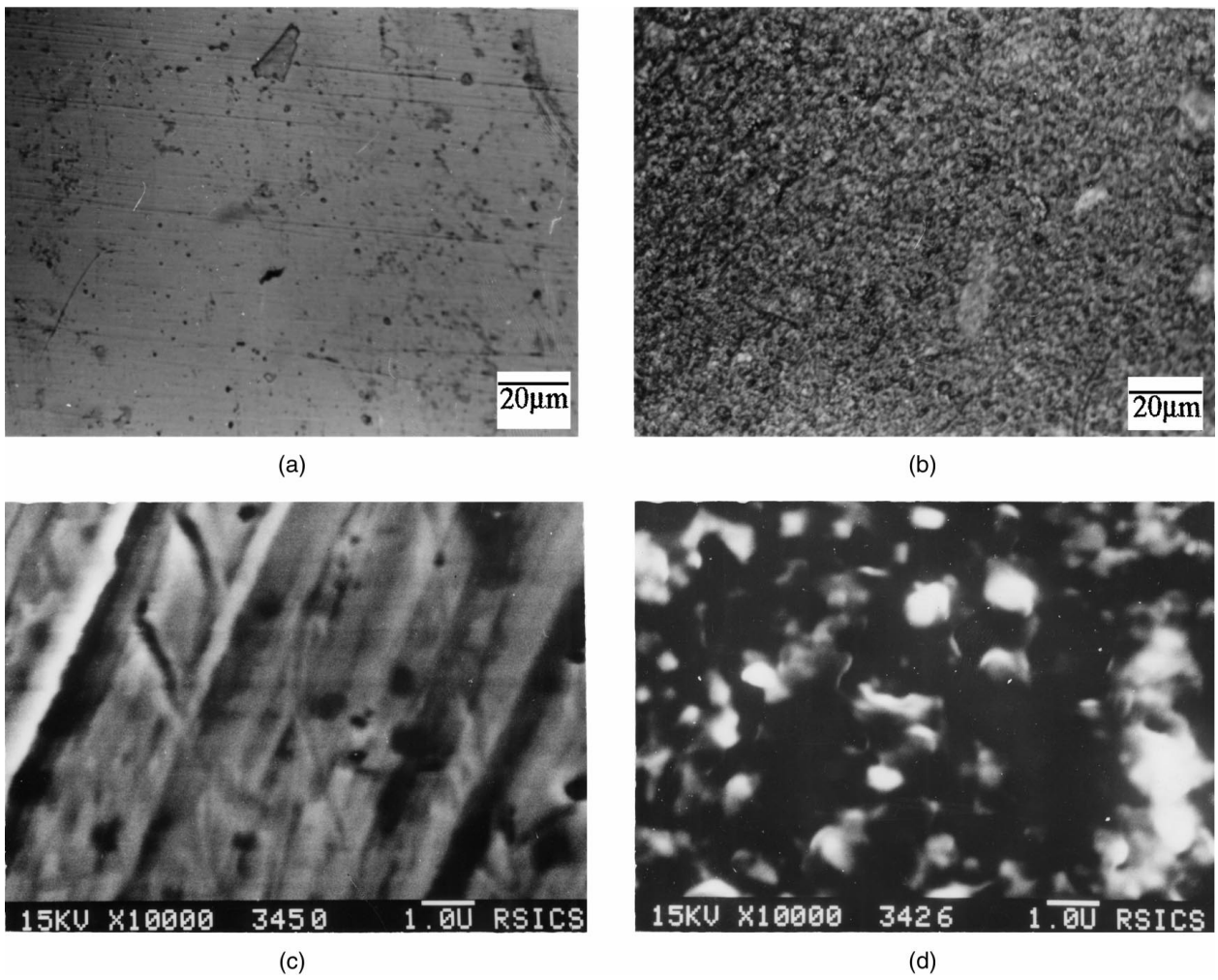

Figure 2 (a) Optical micrograph of un-nitrided SS 302 surface, magn. 500×. (b) Optical micrograph of plasma ($Ar : N_2 : H_2 = 1 : 1 : 3$) nitrided SS 302 surface, magn. 500×. (c) SEM micrograph of un-nitrided SS 302 surface, magn. 10,000×. (d) SEM micrograph of plasma ($Ar : N_2 : H_2 = 1 : 1 : 3$) nitrided SS 302 surface, magn. 10,000×.

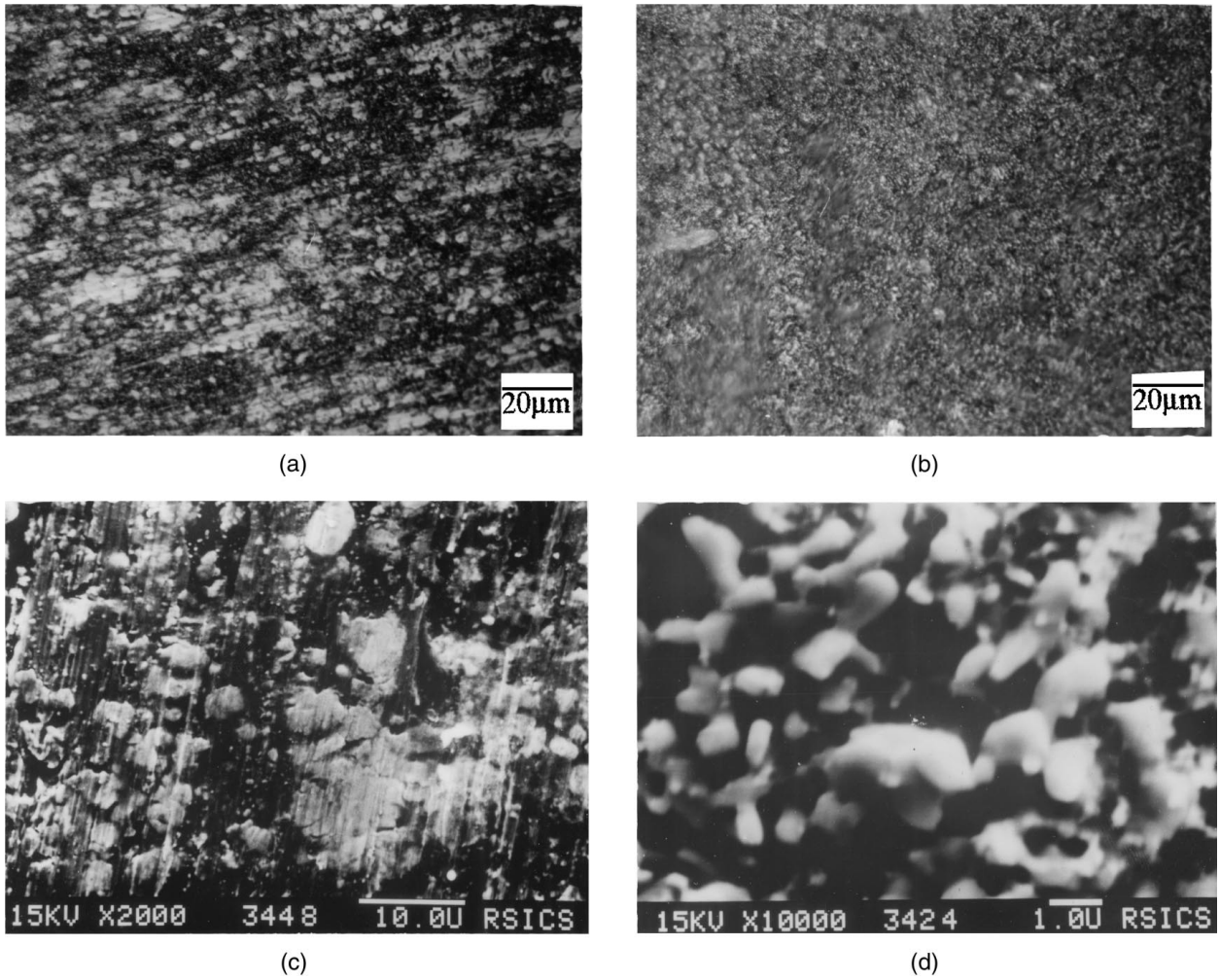

Figure 3 (a) Optical micrograph of un-nitrided HCS surface, magn. 500×. (b) Optical micrograph of plasma ($Ar : N_2 : H_2 = 1 : 1 : 3$) nitrided HCS surface, magn. 500×. (c) SEM micrograph of un-nitrided HCS surface, magn. 2000×. (d) SEM micrograph of plasma ($Ar : N_2 : H_2 = 1 : 1 : 3$) nitrided HCS surface, magn. 10,000×.

conditions. The grain morphologies of SS 302 and HCS after nitridation look similar to 500× magnification. It was also observed that change of plasma from Ar-N_2-H_2 to Ar-N_2 does not change the grain morphologies. SEM studies of the above samples reveal the microstructures of the surfaces in Fig. 2c and d and Fig. 3c and d in more detail at higher magnification and corroborate the results obtained in optical microscopy. At 10,000× magnification the spheroidised nitrided surface grains of SS 302 are clearly seen in (SEM) micrograph shown in Fig. 2d vis-a-vis un-nitrided surface grain morphology in Fig. 2c which is marked with some unpolished micro-ridges. The SEM microstructures of HCS observed at two different magnifications are compared in Fig. 3c and d. The morphology of the surface structure [Fig. 3d] appears to have some resemblance with sorbite like pearlite structure which could have grown on substrate surface due to carbon contamination from graphite electrode. By viewing the cross-section of the substrate through SEM the thickness of nitride layer on SS 302 and HCS substrates was determined and it was found to lie between 40–50 μm for both SS 302 and HCS.

The microhardness results of the nitrided and un-nitrided SS 302 and HCS substrates are shown in Table IV. The hardness of HCS is found to be more than that of SS 302 in un-nitrided condition but after nitridation SS 302 exhibits higher hardness than HCS. The hardness for SS 302 increases three to four times after arc plasma nitriding while in HCS it does not increase more than two times.

TABLE IV Micro-hardness of SS 302 and HCS substrates before and after plasma nitriding

	Experimental condition	Micro-hardness[a] SS 302	(HVN) (100 g load) HCS
I	No treatment with any plasma	234	391
II	Treated with Ar plasma	706	450
III	Treated with Ar-N_2 plasma (1 : 5)	914	772
IV	Treated with Ar-N2-H2 plasma (1 : 1 : 3)	872	694

[a]Average of five different readings taken over the central area of the surface of the specimens.

4. Discussion

In thermal plasma which is produced at 10^5 Pa and above pressure in a furnace, the ion density is very high

($\geq 10^{14}$ per cm^3). No direct method other than the pyrometric (spectrometric) method would work in this range due to an inherent limitation of each technique used for temperature measurement and also for limitation posed by the structure of a furnace. The pyrometric technique used by us to monitor the surface temperature of SS 302 and HCS samples is basically an IR spectrometric technique operating in the wavelength range of 0.8–1.1 μm. While calibrating the pyrometer we have observed that it records more accurate result if the plasma was momentarily extinguished in the furnace at the time of focussing the pyrometer on the substrate. Hence in all our arc plasma nitriding experiments such procedure was followed to determine the temperatures as given in Tables II and III. The substrate temperature is seen to differ by 5–10 °C from SS 302 to HCS which could be due to absence of exact data on emissivity (e) for these two materials. In our measurement we have taken $e = 0.28$ for both SS 302 and HCS. The substrate temperature is also seen to vary from Ar to Ar-N_2 to Ar-N_2-H_2 plasma under similar current-voltage condition which may be attributed to the lower heat capacity of Ar ($C_p = 20.72\ J\,m^{-1}\ K^{-1}$) and higher enthalpy of hydrogen.

Traditional industrial nitriding process of steel surfaces is carried out either by N_2 or NH_3 gas nitriding process in the temperature range 450–650 °C or by a cyanide-cyanate salt bath between 800–950 °C. Plasma nitriding processes recently adopted to surface engineering industries of steel components hardly exceed 600–650 °C substrate temperature in dc glow discharge method in order to avoid distortion and drop in structural hardness of steel. In literature [7–9, 24] uptill now no attempt seems to have been made to nitride steel substrates in an unusual high temperature range, 1100–1200 °C. The case depth or nitride layer thickness in both SS 302 and HCS observed by us (in SEM) are found to be of the order of 40–50 μm in just 20 min time of exposure which is unusually high. The thickness, however, is found to be quite smaller than the value (1.15 mm) calculated on the basis of activation energy 1.45 eV/atom (in austenite stainless steel (fcc)) fitted by Williomson *et al*. [10] from a wide range of plasma nitrided and ion beam implanted samples in the temperature range 350–450 °C. With addition of H_2 in Ar-N_2 plasma, the growth rate of nitride layer was not found to change which is similar to the findings of Renevier *et al*. [11] in case of low pressure arc plasma. In view of high growth rate in the arc plasma nitriding, the process is quite amenable to industrial nitriding of SS and HCS.

XRD results shown in Table II and III reveal the various phases identified in SS 302 and HCS surfaces without and with plasma treatment. While $Fe_{2-3}N(\varepsilon)$ and $(Cr, Fe)_2N_{1-x}$ have been found to be the two common major phases to grow after Ar-N_2 and Ar-N_2-H_2 plasma treatment on SS 302 and HCS surfaces, austenite SS and HCS are the phases that grow after Ar plasma treatment. The spectacular difference one can mark between SS 302 and HCS is that CrN appears as a new major phase in the SS but in HCS it is totally absent. WN and $Fe_2N(\varepsilon)$ are seen to occur as the other major phases in the HCS. It is observed that iron oxide in various phases gives minor reflections in case of all plasma treated samples. This may be ascribed to the presence of oxygen in plasmagen gas used and residual oxygen in the furnace due its semi-open structure. The occurence of $Fe_{2-3}N(\varepsilon)$ as a minor phase for the case of Ar plasma treated SS and HCS samples may also be attributed to the semi-open nature of furnace where N_2 from residual air causes the formation of the most common nitride phase. It is quite surprising that no carbide reflection due to Fe and W are observed in XRD in case of plasma treated HCS samples in spite of their strong chemical affinity with carbon. Similarly any nitride phase containing Ni is also found missing for the case of plasma treated SS 302 samples due to stronger affinity of Fe for N than Ni for N. Such a view has been recently experimentally confirmed by Ima and others [12] in case of ion implanted Ni/Fe bilayer where XRD and TEM identified the formation of $Fe_{3-x}N$ in the lower Fe layer.

Visual observation of the arc plasma nitrided SS 302 and HCS samples reveals the surfaces to be smooth but dotted with few uneven or rough spots like the hot spots in dc glow discharge plasma nitriding. As we have prepared the samples in the non-transferred mode of arc plasma and the arc length was small (1.0–1.5 cm) compared to the distance between nitriding specimens and arc zone (~3 cm), the possibility of hot spot formation due to side arcing is remote. However, since nitriding was carried out in a graphite arc plasma, carbon (vapours) emanating from the arc might have caused some localised rough spots on the substrate surface by mechanical adhesion and/or diffusion. Surface morphology of the nitrided and un-nitrided samples viewed under an optical microscope is shown in Figs 2a, b and 3a, b and reveals the typical microstructures of SS 302 and HCS surfaces respectively. The morphology is seen to be similar to the observation of Cocke *et al*. [13] for the case of SS samples nitrided by rf plasma (80 MHz, 1.6 Torr) and identified as due to $Fe_{2-3}N(\varepsilon)$ phase produced after 15 min of plasma treatment in a $1:3\ N_2:H_2$ plasma. Tosic and Gligorijevic [14] also reported the growth of a $Fe_{2-3}N(\varepsilon)$ layer by dc glow discharge plasma (80% N_2, 20% H_2) exhibiting surface morphology like ours for the case of 42 CrMO4 steel components. The fact that surface morphology of only $Fe_{2-3}N(\varepsilon)$ phase is observed by us in optical microscope suggests that other major phases such as $(Cr, Fe)_2N_{1-x}$, CrN, Fe_2N etc. (identified in XRD) do not lie in the top surface, rather they grow below $Fe_{2-3}N(\varepsilon)$ layer. The SEM pictures taken at higher magnifications show the surfaces and grains of un-nitrided and nitrided SS 302 and HCS in Figs 2c, d and 3c, d respectively. The spheroidised nitride grain structures of SS 302 vis-a-vis un-nitrided SS 302 surface morphology characterised with micro-ridges have been compared in Fig. 2d and c. The microstructures of HCS with and without nitriding shown in Fig. 3d and c clearly distinguish between grains of nitride (resembling sorbite like pearlite) and austenite.

Microhardness is an index to ascertain the presence of hard phase like carbide, nitride etc. in any surface. The results of Vicker's microhardness tests conducted on the

un-nitrided and arc plasma nitrided samples are shown in Table IV. The hardness values have been determined on 40–50 μm nitride layer thickness. The Vicker's hardness number increases up to a maximum of 914 for SS 302 and 772 for HCS from respective initial values of 234 and 391 for un-nitrided samples and the highest hardness is achieved in case of Ar-N_2 plasma at $Ar : N_2 = 1 : 5$ which suggests a diffusion controlled process to operate. This view appears to be tenable in view of the relatively low hardness value attained in our nitrided SS 302 and HCS samples indicating the absence of $Fe_4N(\gamma')$ phase (5.7–6.1% N) which produces high hardness due to its cubic lattice. The XRD results (Tables II and III) and surface morphology observed under microscope (Figs 2 and 3) (reveal $Fe_{2-3}N$ (ε) grows on the surface layer followed by other phase growths in the underlying layer) also corroborate the above diffusion controlled nitriding process. As shown in Table II and III the ar plasma nitriding has been carried out in an unusual high temperature range 1100–1200 °C in which SS 302 and HCS lattice would soften and allow more inter atomic and interstitial diffusion of nitrogen. It may thus be reasoned out that the appearance of high nitrogen phase such as Fe_2N (11.35% N), $Fe_{2-3}N$ (8–11.2% N), WN, CrN etc. as major phases and growth of high thickness case (40–50 μm) in 20 min are caused due to enhanced nitrogen diffusion.

In the nitriding process a major controversy as to the nature of nitrogen species diffusing into iron still remains unresolved. In the gas nitriding and cyanide-cyanate liquid nitriding process it is reported [15] that atomic nitrogen (N) diffuses into iron from surface and forms various kinds of nitride phases at different depths. In plasma nitriding the scenario is confusing due to different kinds of species reported in spectroscopic studies. The roles of N_2 and N_2^+ were studied by Henrion and co-workers [16–19] from optical emission studies in N_2 and N_2-H_2 plasma discharges but no conclusion could be arrived at due to process dependence of concentration of the species. Spectroscopic studies in triode [20], high current arc discharge [9] and dc glow discharge plasma [21, 22] also could not resolve the issue. The concentrations of ion and neutral species are however reported to show different trends in microwave plasma [22] when hydrogen is added. In the arc plasma used in our nitriding furnace the central temperature zone (arc zone) does not exceed 7000 °C. Following literature [23] one can have some idea about the concentration of nitrogen species in nitrogen plasma furnace at such temperature at atmospheric pressure ($\sim 10^5$ Pa). The respective numbers of the species are as follows:

$$N_2 = 4.10 \times 10^{21} \qquad N = 6.40 \times 10^{21}$$
$$N^- = 1.40 \times 10^{14} \qquad N_2^+ = 5.50 \times 10^{17}$$
$$N^+ = 3.40 \times 10^{18} \qquad e = 3.90 \times 10^{18}$$

It is evident that the concentrations of N_2 and N are higher by around 10^4 times than that of N_2^+, 10^3 times than that of N^+ and e (electron), and 10^7 times than that of N^-. The data may not exactly predict the situation in the nitrogen plasma furnace used in our case but certainly gives some idea about the species participating more in the nitriding process. In the light of the above logic one could infer that excited N_2 and atomic N play a dominant role in arc plasma nitriding.

5. Conclusion

Arc plasma nitriding of SS 302 and HCS surfaces carried out in the high temperature range 1100–1200 °C produces $Fe_{2-3}N(\varepsilon)$ and mixture of other nitride phases along with small amounts of oxides of iron. The cubic phase [$Fe_4N(\gamma')$] which produces highest hardness in iron is not marked to grow in this process. High growth rate of the nitride layer (40–50 μm in 20 min) coupled with lesser high hardness value of the nitrided grains suggests an accelerated rate of nitrogen diffusion taking place in the softened surface of steel at high temperature. Excited N_2 and atomic N seem to dominate in the arc plasma nitriding process. The process being amenable can be easily extended to plasma flame nitriding using an arc plasma torch to provide erosion and corrosion resistant nitride coating at typical location of large structure components for long service life.

References

1. K. MAENOSONO and A. ISHIBISHI, *J. Soc. Mater. Sci., Jpn.* **44** (1995) 782.
2. F. EL-HESSARY, F. MOHAMAD, F. HENDRY, D. J. FABIAN and Z. SZASZNE-CSIH, *Surf. Engg.* **4**(2) (1988) 150.
3. A. M. TAYLOR, "Adv. Vac. Sys." (Ayer, MA 1980).
4. Z. L. ZHANG and T. BELL, *Surf. Engg.* **1** (1985) 131.
5. J. P. LEBRUN, H. MICHEL and M. GANTOIS, *Mem. Etud. Sci. Rev. Metall.* **69** (1972) 727.
6. R. URAO, K. YAMAGATA and H. YOSHIDA, in Proc. 7th Int. Conf. on Vacuum Metallurgy (1982) p. 584.
7. M. J. BALDWIN, G. A. COLLINS, M. P. FEWELL, S. C. HAYDON, S. KUMAR, K. T. SHORT and J. TENDYS, *Jpn. J. Appl. Phys.* **36** (1997) 4941.
8. D. S. STAVREV, L. M. KAPUTKINA, S. K. KIROV, YU. V. SHAMONIN and V. G. PROKOSHKINA, *Metalloved. Term. Obrab. Met.* **9** (1996) 16.
9. N. RENEVIER, P. COLLINGNON, H. MICHAL and T. CZERWIEC, *Surf. Coat. Technol.* **86**(7) (1996) 285.
10. D. L. WILLIAMSON, O. ÖZTÜRK, R. WEI and P. J. WILBUR, *Surf. Coat. Technol.* **65** (1994) 15.
11. N. RENEVIER, T. CZERWIEC, P. COLLINGNAN and H. MICHEL, *ibid.* **98**(1–3) (1998) 1400.
12. D. K. IMA, F. D. TRICHELAAR, W. M. ARNOLDBIK, A. M. VERDENBERG and D. O. BOERMA, *J. Mater. Res.* **13**(2) (1998) 440.
13. D. L. COCKE, M. JURCIK-RAJMAN and S. VEPREK, *J. Electrochem. Soc.* **136**(12) (1989) 3655.
14. M.M. TOSIC and GLIGORIJEVIC, in "Plasma Surface Engg.," edited by E. BROSZCIT, W. D. MUNZ, H. OICHSNER, K.-T. RIE and G. K. WOLF, (DGM Informationsgesellschaft. Verlag, Bonn, Germany, 1989) pp. 903.
15. YU. M. LAKHTIN, Engg. "Physical Metallurgy and Heat Treatment" (Mir Publ. Moscow, 1979) pp. 274, 280.
16. J. BOUGODIRA, G. HENRION and M. FABRY, *J. Phys. D* **24** (1991) 1076.
17. J. BOUGODIRA, G. HENRION and M. FABRY, M. REMY and R. CUSSENOT, *Mater. Sci. Engg. A* **139** (1991) 15.
18. G. HENRION, M. FABRY, R. HUGON and J. BOUGODIRA, *Plasma Sources Sci. Technol.* **1** (1992) 117.

19. R. HYUGON, M. FABRY and G. HENRION, *J. Phys. D* **29** (1996) 761.
20. J. D. HAEN, C. QUAEYHAEGENS, G. KNUYT, M. D. OLIESLAEGER and L. M. STALS, *Surf. Coat. Technol.* **74**(5) (1995) 405.
21. K. RUSRAK and J. VLCEK, *J. Phys. D* **26** (1993) 585.
22. S. BOCKEL, J. AMORIM, G. BARAVIAN, A. RICARD and P. STRATIL, *Plasma Sources Sci. Technol.* **5** (1996) 567.
23. V. DEMBOVOSKY, "Plasma Metallurgy, The Principles," (Elsevier Publ. Amsterdam, 1985) pp. 84.
24. W. D. FAY, PCT Int. Appl. WO 97 14, 820 (cl.c.23c8/28), 24 Apr., 1997.

Received 21 October 1998
and accepted 5 May 1999